

29. D. R. Jennison, A. Bogicevic, *Surf. Sci. Lett.* **464**, 108 (2000).
 30. A. E. Mattsson, D. R. Jennison, in preparation.
 31. L. A. Curtiss, K. Raghavachari, G. W. Trucks, J. A. Pople, *J. Chem. Phys.* **94**, 7221 (1991).
 32. The endothermic reaction $2\text{OH}^- + \text{Co}^0 \rightarrow \text{O}^{2-}\text{Co}^0 + \text{H}_2\text{O}$ does not produce Co(II).
 33. G. Mills, H. Jonsson, G. K. Schenter, *Surf. Sci.* **324**, 305 (1995).
 34. The LDA binding energy (1.08 eV) is likely below the real value (28). Estimating the surface self-energy correction (30) produces this estimate. In addition, the thermal energy of the source contributes 0.11 eV.
 35. J. Strömquist *et al.*, *Surface Science*, **397**, 382 (1998).
 36. M. Persson *et al.*, *J. Chem. Phys.* **110**, 2240 (1999).
 37. K. C. Hass, W. F. Schneider, A. Curioni, W. Andreoni, *J. Phys. Chem. B* **104**, 5527 (2000).
 38. We thank R. R. Stumpf for critical comments and J. Strömquist for useful discussions. Pacific Northwest National Laboratory (PNNL) and Sandia National Laboratory (SNL) are multiprogram laboratories operated for the U.S. Department of Energy by Battelle Memorial Institute under Contract DE-AC06-76RLO 1830 (PNNL), and by Sandia Corporation, a Lockheed Martin Company, under Contract DE-AC04-94AL85000 (SNL). The

experimental work was conducted in the Environmental Molecular Sciences Laboratory, a national scientific user facility sponsored by the Department of Energy's Office of Biological and Environmental Research and located at PNNL. T.R.M. acknowledges the Motorola/SNL computational materials Cooperative Research and Development Agreement. S.A.C. and T.D. were supported by the U.S. Department of Energy, Office of Science, Office of Basic Energy Sciences, Division of Materials Science at PNNL.

30 April 2002; accepted 14 June 2002

Detection of a Large-Scale Mass Redistribution in the Terrestrial System Since 1998

Christopher M. Cox^{1*} and Benjamin F. Chao²

Earth's dynamic oblateness (J_2) had been undergoing a decrease, according to space geodetic observations over the past 25 years, until around 1998, when it switched quite suddenly to an increasing trend that has continued to the present. The secular decrease in J_2 resulted primarily from the postglacial rebound in the mantle. The present increase, whose geophysical cause(s) are uncertain, thus signifies a large change in global mass distribution with a J_2 effect that considerably overshadows that of mantle rebound.

Earth's mean tide-free dynamic oblateness (J_2) $\equiv [C - (A + B)/2]/MR^2 = 1.082627 \times 10^{-3}$, where $C > B \geq A$ are Earth's mean principal moments of inertia and M and R are the mean mass and radius, respectively. Satellite laser ranging (SLR) has yielded precise determination of the temporal variation in the low-degree spherical harmonic components of Earth's gravity field, beginning with the initial observations of J_2 change made by observing Lageos-1 satellite orbital node accelerations (1, 2). More recent studies have extended the knowledge to higher degree zonals and examined the annual signals in the low-degree geopotential (3–5). The estimated values of the J_2 rate have ranged from -2.5×10^{-11} year⁻¹ to -3×10^{-11} year⁻¹.

The extension of comprehensive solutions for low-degree geopotential zonal, static, annual, and rate terms and the 9.3- and 18.6-year ocean tide amplitudes to include data since 1997 has resulted in increasingly significant changes in the estimated J_2 rate and 18.6-year tide amplitude (4). These changes implied that the models for these terms were not accommodating the observed signal. Consequently, we estimated a time series of low-degree (maximum degree of 4) static geopotential solutions using SLR observations of 10 satellites over the period from

1979 to 2002. The inclusion of multiple orbital inclinations improves separation of the higher degree zonal components and allows recovery of the gravity coefficients over shorter time periods. All processing used the same algorithms used to develop the EGM96S satellite-only gravity model and to calibrate that model's covariance (5). The 18.6-year and much smaller 9.3-year tide amplitudes were set to the values estimated in the comprehensive solution with data from 1979 through 1997 (4). The applied 18.6-year tide amplitude of 1.41 cm has the equivalent J_2 amplitude of 1.67×10^{-10} . The 18.6-year tide- J_2 effect is minimized (that is, the geopotential is less oblate) when the lunar node is 0 degrees, which occurred in mid-October 1987.

Shown in Fig. 1 is the estimated J_2 as a function of time, $J_2(t)$. Lageos-1 data are present throughout, and Starlette data are present from January 1980 onward. Data completeness issues precluded the use of the earlier Starlette and Lageos-1 data. Other satellites were added when launched: Ajisai from August 1986 and Lageos-2 and several other satellites from 1992 onward. TOPEX/POSEIDON (T/P), which is also tracked by the Détermination d'Orbite et Radiopositionnement Intégrés par Satellite system, was added in January 1993. The formal uncertainties shown reflect the SLR data weights derived from the calibration of the comprehensive 19-year solution and should be realistic (6).

Dominant in $J_2(t)$ is a seasonal signal of

amplitude 3.2×10^{-10} , which is driven by meteorologic mass redistribution in the atmosphere-hydrosphere-cryosphere system (7–10). Also plotted in Fig. 1 is the atmospheric contribution calculated according to the National Center for Environmental Prediction (NCEP) reanalysis data (11), including the inverted-barometer (IB) correction (12). Subtraction of this signal and further empirical removal of the residual seasonal signals (which are attributable to the poorly known seasonal mass redistribution in the oceans and land hydrology) result in a nonatmospheric and nonseasonal $J_2(t)$ (Fig. 2).

A linear fit to the observed J_2 through 1996 shows a decrease in J_2 of -2.8×10^{-11} year⁻¹ (Fig. 2). For this period, the uncertainty for the J_2 rate in the comprehensive solution (which considers the correlation with the 18.6-year tide) is 0.4×10^{-11} year⁻¹. Despite the lack of data before 1979, the results are in excellent agreement with estimates of the J_2 rate that included those data (2). The secular drift results primarily from postglacial rebound (PGR) (2, 13, 14) in the mantle, plus various secondary contributions of climatic and anthropogenic origin (for example, reservoirs, which are an order of magnitude too small to explain the recent observations) (4, 15, 16). At some time during 1997 or 1998, the trend reversed. The post-1996 points have deviated from the pre-1997 slope by about six times the uncertainties, on average, over that period. A linear fit from 1997 onward yields a rate of $+2.2 \times 10^{-11}$ year⁻¹. On the basis of the comprehensive solutions, the uncertainty for this rate is $\sim 0.7 \times 10^{-11}$ year⁻¹; however, because of the nonlinearity in $J_2(t)$, the slope can vary by more than the uncertainty value, depending on the period fitted. Another departure may exist around 1980, but excepting a few data points the deviation is only one to two times the uncertainties, making the importance unclear.

An increase in J_2 means a net transport of mass from high to low latitude (the nodal lines of J_2 are $\pm 35.3^\circ$ latitude). Transport of terrestrial water and/or ice mass to the oceans is one likely cause, because most of the ice mass resides in high-latitude polar caps and glaciers. As an example of the mass flux involved, imagine one fictitious scenario that

¹Raytheon Information Technology and Scientific Services (ITSS), ²Space Geodesy Branch, NASA Goddard Space Flight Center, Code 926, Greenbelt, MD 20771, USA.

*To whom correspondence should be addressed. E-mail: ccox@stokes.gsfc.nasa.gov

would increase J_2 : a uniform melting of the Greenland ice sheet, resulting in an eustatic global sea level (GSL) rise. For every 10^{-11} increase of J_2 , the required loss of Greenland mass as the water volume equivalent is 102 km^3 , accompanied by a 0.28-mm increase in GSL (15). To overshadow PGR and produce a change comparable to that in the observed J_2 rates, nearly five times as much water mass is necessary, amounting to $\sim 1.4 \text{ mm year}^{-1}$ in additional GSL rise. This is a global change of huge proportions that has not been observed in modern times (17).

Ice height changes over Greenland have been observed with radar and laser altimetry (18, 19). However, the net ice height and implied GSL changes (about $\pm 0.2 \text{ mm year}^{-1}$) are too small to explain the changes in the observed J_2 . We calculated the $J_2(t)$ for the Greenland plus West Antarctica ice height estimates using ERS-1 and -2 satellite altimetry data (19) up to 81.4°N and S (Fig. 2). Again, the magnitude is too small; and if anything, the ice height variation implies a mass transport that is opposite of the observed anomaly.

Recent studies indicated an acceleration of the mass wastage of mountain glaciers (20, 21). The average loss rate for the subpolar glaciers had been $\sim 100 \text{ km}^3$ of water per year before 1997, with accelerated rates in the

past decade (21). For the observed J_2 rate change to be explained by additional glacier mass loss, an additional water mass loss of $\sim 700 \text{ km}^3$ per year would be required. The resultant GSL increase of 2.0 mm/year over the pre-1998 rate has not been observed (22). It is unlikely that transport of terrestrial water mass to the oceans can explain the J_2 changes; however, more recent glacier and ice height data are needed to definitively rule this out.

Mass redistribution within the oceans could cause a net J_2 change with little or no GSL signature. The calculated $J_2(t)$ due to the apparent GSL variation within $\pm 66^\circ$ latitude according to the T/P GSL data (23), assuming geographically uniform mass addition, is given in Fig. 2. This calculation overestimates the J_2 effect because much of the observed GSL variation is steric (24, 25), especially at low latitudes. Even so, the change in the GSL-implied J_2 before and after the strong 1997–98 El Niño is too small to account for the J_2 observations. Also shown is the J_2 signature calculated from the actual geographic distribution of the sea surface height changes (23) (again assuming no steric contributions) after removal of an empirical annual term. The slope after 1999, when the sea surface temperature had returned to normal after the 1997–98 El Niño, is consistent and

comparable with the observed J_2 , suggesting that oceanic mass transport could be responsible without having a substantial signature in GSL. Further research is needed and in progress. It is intriguing to consider the possibility of a different climatic mass distribution state (17) triggered by the strong 1997–98 El Niño event. For example, the melting of polar sea ice, which has no direct effect on J_2 , can cause as-yet-unknown changes in the thermohaline circulation and structure, and therefore indirectly J_2 , as a result of the melting of the insulating freshwater sea ice layer over the Arctic Ocean (17).

So far $J_2(t)$ is the only gravity-time record in which we have found unequivocal evidence for the anomalous mass redistribution. The higher degree zonals, such as $J_3(t)$ (figs. S1 and S2) and $J_4(t)$ (figs. S3 and S4), do show interannual fluctuations, but it is unclear whether these data show similar systematic change. A lack of change in J_3 would mean that there was no net north-south mass redistribution. Earth rotation records, both length-of-day and polar motion, are potentially useful for delineating global mass transports. However, interpretation of these records is complicated by the interannual signals, which are dominated by dynamic processes within Earth's core.

Judging from the large magnitude and relatively rapid evolution of the observed J_2 changes, one possible cause could be net material flow driven by the geodynamo in the fluid outer core and along the core-mantle boundary. There is evidence of a substantial geomagnetic jerk in 1999. Such jerks have been associated with flow acceleration in the top of the core (26, 27), in addition to long-term magnetic dipole changes. Could they be related? To date, no correlation has been demonstrated between the geomagnetic observations and the observed $J_2(t)$. However, a review of geodynamo simulation results (28) indicates that the core models can possibly explain J_2 changes at the level of $0.1 \times 10^{-11} \text{ year}^{-1}$ to $0.5 \times 10^{-11} \text{ year}^{-1}$, depending on the modeling assumptions.

In principle, climatic general circulation models (GCMs), especially models coupling the atmosphere-ocean-cryosphere with land hydrology, can help to explain the J_2 changes. Indeed, some secondary interannual variability in J_2 is presumably climatic (Fig. 1). However, traditional GCMs simply do not have sufficient physics or knowledge built into their climatic feedback mechanisms to anticipate sudden changes (17) such as the recent observed J_2 changes. Further, GCMs are almost invariably too conservative and tend to underestimate the climatic variability when compared with in situ and ground truth data, because of insufficient resolution in the numerical computation (17, 29–31).

Fig. 1. J_2 variation observed by SLR as compared with the IB-corrected NCEP atmospheric J_2 . The atmospheric series (top) is on the left scale, and the observed series (bottom) is on the right scale. Sampling intervals are 90 days in 1979, 60 days from 1980 through 1991, and 30 days afterward. No detrending has been performed. Units are $\times 10^{-10}$.

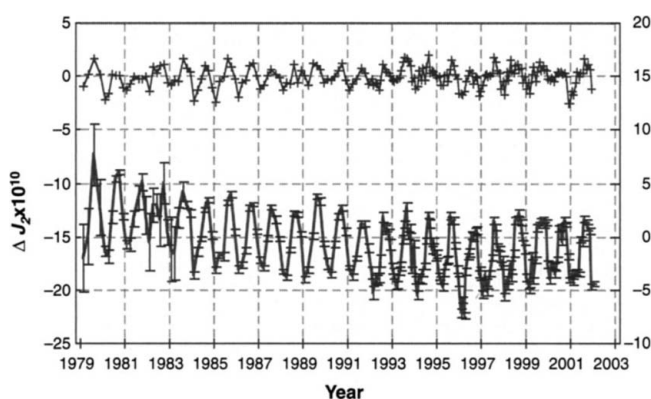
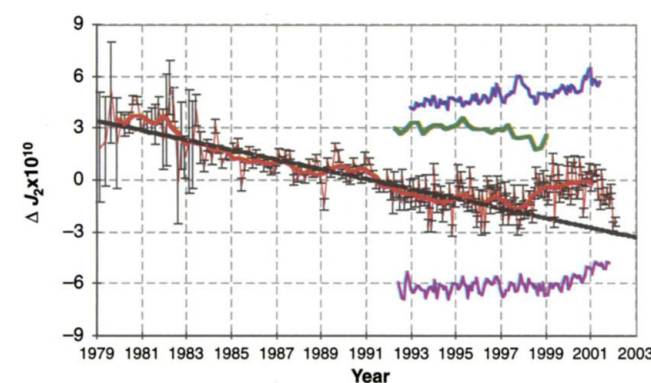


Fig. 2. Observed J_2 , after subtraction of the IB-corrected atmospheric signal and an empirical annual term before (thin red line) and after (heavy red line) an annual filter has been applied. Error bars are the observed J_2 uncertainties. The black line is a weighted fit to the (unfiltered) pre-1997 data. The slope is $-2.8 \times 10^{-11} \text{ year}^{-1}$. The offset green line is the J_2 implied by the Greenland plus West Antarctic ice heights derived from ERS-1 and ERS-2 altimetry data. Also shown are the J_2 value implied by the T/P uniform GSL change (blue, offset) and the J_2 value when the geographic distribution of the sea height changes is considered (purple, offset). Neither sea height-derived estimate includes steric effects. Units and sampling intervals are as in Fig. 1.



References and Notes

1. C. F. Yoder *et al.*, *Nature* **303** 757 (1983).
2. D. P. Rubincam, *J. Geophys. Res.* **89**, 1077 (1984).
3. M. K. Cheng, C. K. Shum, B. D. Tapley, *J. Geophys. Res.* **102**, 22377 (1997).
4. C. M. Cox, S. M. Klosko, B. F. Chao, in *Gravity, Geoid and Geodynamics 2000: International Association of Geodesy Symposium*, M. Sideris, Ed. (Springer-Verlag, Heidelberg, Germany, 2002), vol. 123, pp. 355–360.
5. F. G. Lemoine *et al.*, *NASA Technical Publication 206861* (NASA Goddard Space Flight Center, Greenbelt, MD, 1998).
6. These weights correspond to a data uncertainty of about 1 to 2 m for the SLR data (4), which is 10 to 20 times larger than the data performance. This is representative of the uncertainties generally derived in gravity model development (5) and appears to be the result of limitations in the forward modeling and solution parameterization.
7. R. S. Nerem *et al.*, *Geophys. Res. Lett.* **27**, 1783 (2000).
8. B. F. Chao, W. P. O'Connor, *Geophys. J.* **94**, 263 (1988).
9. B. F. Chao, A. Y. Au, *J. Geophys. Res.* **96**, 6577 (1991).
10. A. Cazenave *et al.*, *Earth Planet. Sci. Lett.* **171** 549 (1999).
11. Data from the National Center for Environmental Prediction, National Oceanic and Atmospheric Administration, are available at http://wesley.wvb.noaa.gov/cdas_data.html.
12. The IB is a correction for a fluid-loading effect that assumes that the ocean surface height responds isotropically to overlying atmospheric pressure. It is most accurate at large spatial scales and time periods longer than weeks, which are applicable to this analysis. For reference see C. Wunsch, D. Stammer, *Rev. Earth Planet. Sci.* **26**, 219 (1998).
13. J. X. Mitrovica, W. R. Peltier, *J. Geophys. Res.* **98**, 4509 (1993).
14. D. Han, J. Wahr, *Geophys. J. Int.* **120**, 287 (1995).
15. T. S. James, E. R. Ivins, *J. Geophys. Res.* **102**, 605 (1997).
16. B. F. Chao, *Geophys. Res. Lett.* **22**, 3529 (1995).
17. National Research Council, *Abrupt Climate Change*, R. Alley, Ed. (National Academy Press, Washington, DC, 2001). This comprehensive report calls attention to modern findings regarding past abrupt climate changes, the most notable of which occurred over periods of just a few years.
18. W. Krabill *et al.*, *Science* **289**, 428 (2000).
19. Results were provided by J. Zwally (Goddard Space Flight Center), using techniques described by J. Zwally, A. Brenner, in *Altimetry and Earth Science*, L. L. Fu, A. Cazenave, Eds. (Academic Press, London, 2001) pp. 351–369.
20. For example, see A. A. Arendt, K. A. Echelmeyer, W. D. Harrison, C. S. Lingle, V. B. Valentine, *Science* **297**, 382 (2002).
21. M. Dyurgerov, M. Meier, *Proc. Natl. Acad. Sci. U.S.A.* **97**, 1406 (2000).
22. The modern GSL rise is estimated to be 1.5 to 2 mm/year [B. Douglas, M. Kearney, S. Leatherman, Eds., *Sea Level Rise* (Academic Press, San Diego, CA, 2001)]. It is due to the steric (thermal plus salinity) effect plus the water mass addition.
23. Results were provided by the NASA Ocean Altimeter

Pathfinder Project and are available at <http://lilia.gsfc.nasa.gov/ocean.html>.

24. S. Levitus, J. I. Antonov, T. P. Boyer, C. Stephens, *Science* **287**, 2225 (2000).
25. C. Cabanes, A. Cazenave, C. Le Provost, *Science* **294**, 840 (2001).
26. M. Alexandrescu, D. Gilbert, G. Hulot, J. L. Le Mouél, G. Saracco, *J. Geophys. Res.* **101**, 21975 (1996).
27. M. Manda, E. Bellanger, J. L. Le Mouél, *Earth Planet. Sci. Lett.* **183**, 369 (2000).
28. Results provided by W. Kuang (University of Maryland Joint Center for Earth Technology), based on models described in W. Kuang, J. Bloxham, in *The Core-Mantle Boundary Region*, M. Gurnis *et al.*, Eds. (AGU, Washington, DC, 1998) pp. 197–208.
29. L. L. Fu, R. D. Smith, *Bull. Am. Meteorol. Soc.* **77**, 2625 (1996).
30. D. R. Stammer *et al.*, *J. Geophys. Res.* **101**, 25779 (1996).
31. T. J. Johnson, C. R. Wilson, B. F. Chao, *J. Geophys. Res.* **106**, 11315 (2001).
32. We thank A. Au and J. Beall of Raytheon ITSS for their data-processing assistance. We have benefited from discussions with M. Cheng, R. Eanes, S. Klosko, S. Nerem, E. Ivins, W. Kuang, M. Purucker, and V. Zlotnicki. Supported by NASA's Oceanography Program and Solid Earth and Natural Hazards Program. The SENH program also supports NASA's SLR network.

Supporting Online Material

www.sciencemag.org/cgi/content/full/297/5582/831/DC1
Figs. S1 to S4

25 March 2002; accepted 14 June 2002

Foraminiferal Calcification Response to Glacial-Interglacial Changes in Atmospheric CO₂

Stephen Barker* and Henry Elderfield

A record of foraminiferal shell weight across glacial-interglacial Termination I shows a response related to seawater carbonate ion concentration and allows reconstruction of a record of carbon dioxide in surface seawater that matches the atmospheric record. The results support suggestions that higher atmospheric carbon dioxide directly affects marine calcification, an effect that may be of global importance to past and future changes in atmospheric CO₂. The process provides negative feedback to the influence of marine calcification on atmospheric carbon dioxide and is of practical importance to the application of paleoceanographic proxies.

Higher concentrations of carbon dioxide in the atmosphere cause surface seawater to become more acidic and lower the calcium carbonate saturation state through the consequent decrease in [CO₃²⁻], the carbonate ion concentration (1). Predictions suggest that the carbonate saturation state will be reduced by 30% relative to the preindustrial level by the middle of the 21st century (1, 2). This has raised concern because of evidence that carbonate saturation is correlated with the rate of production of marine calcium carbonate and because of studies showing that coral reefs

and some species of coccolithophorids (major producers of marine carbonate) are sensitive to elevated CO₂ pressure (PCO₂) (3–7). The hypothesis that growth rate is a function of [CO₃²⁻] is also consistent with inorganic studies (8, 9).

If marine calcification is sensitive to the concentration of atmospheric carbon dioxide, its effect should be reflected in the paleoceanographic record as a response to glacial-interglacial fluctuations in PCO₂. Foraminifera constitute an important fraction of marine plankton and play a significant role in the carbon cycle through the production of shell calcite. Increased carbonate ion concentrations in culturing experiments using the planktonic foraminifer *Orbulina universa* have been shown to produce higher shell

weights in similarly sized organisms, interpreted as a consequence of thicker shell walls resulting from higher rates of calcification (10, 11). We have found that shell weights of several species of planktonic foraminifera from core top sediments vary systematically as a function of latitude in the North Atlantic. By combining these findings with a record of shell weight across glacial-interglacial Termination I, we demonstrate that the changes are as a result of ambient [CO₃²⁻] changes rather than calcification temperature and are consistent with known changes in atmospheric PCO₂. The link between marine calcification and [CO₃²⁻] provides a negative feedback to changes in atmospheric PCO₂. This observation is also of practical importance in paleoceanography because shell weight is used as an index of carbonate dissolution at the seafloor and, thus, of past changes in deep-sea [CO₃²⁻] (12).

Measured weights of several planktonic foraminiferal species (picked from narrow size fractions) from a North Atlantic latitudinal transect (13) increase by a factor of about 2 between 60° and 30°N (Fig. 1A). Due to the strong temperature dependence of CO₂ solubility in seawater, and the subsequent dissociation of CO_{2(aq)} into HCO₃⁻ and CO₃²⁻, modern open ocean surface water [CO₃²⁻] varies as a function of temperature. Thus, the observed trend in shell weight would fit with a [CO₃²⁻] control as well as a temperature control. An offset in the shell weights of *Pulleniatina obliquiloculata* and *Neoglobobulimina dutertrei* has been reported between the tropical Atlantic, Indian, and Pacific

Department of Earth Sciences, University of Cambridge, Cambridge CB2 3EQ, UK.

*To whom correspondence should be addressed. E-mail: sbark98@esc.cam.ac.uk